

XMM-Newton observations of the eclipsing polar EP Dra

Gavin Ramsay¹, C. M. Bridge¹, Mark Cropper¹, K. O. Mason¹, F. A. Córdova²

W. Priedhorsky³

¹*Mullard Space Science Laboratory, University College London, Holmbury St. Mary, Dorking, Surrey, RH5 6NT, UK*

²*University of California, Riverside, CA 92521, USA*

³*Los Alamos National Laboratory, MS D436, Los Alamos, NM 87545, USA*

Received:

ABSTRACT

We present *XMM-Newton* observations of the eclipsing polar EP Dra which cover nearly 3 binary orbital cycles. The X-ray and UV data show evidence for a prominent dip before the eclipse which is due to the accretion stream obscuring the accretion region. The dip ingress is rapid in hard X-rays suggesting there is a highly collimated core of absorption. We find that a different level of absorption column density is required to match the observed count rates in different energy bands. We propose that this is due to the fact that different absorption components should be used to model the reprocessed X-rays, the shocked X-ray component and the UV emission and explore the affect that this has on the resulting fits to the spectrum. Further, there is evidence that absorption starts to obscure the softer X-rays shortly after the onset of the bright phase. This suggests that material is threaded by an unusually wide range of magnetic field lines, consistent with the suggestion of Bridge et al. We find that the period is slightly greater than that determined by Schwone & Mengel.

Key words: Stars: individual: – EP Dra – Stars: binaries – Stars: cataclysmic variables – X-rays: stars

1 INTRODUCTION

Polars or AM Her systems are accreting binary systems in which material transfers from a dwarf secondary star onto a magnetic ($B \sim 10\text{--}200\text{MG}$) white dwarf through Roche lobe overflow. They vary in brightness over the binary orbital period, which is synchronised with the spin period of the white dwarf. It has become clear that the accretion flow in these systems is highly variable from one orbital cycle to the next. In eclipsing polars, once the secondary star has completely eclipsed the white dwarf, the accretion flow between the stars is still visible for a short time. In the optical this eclipse profile is seen to vary from cycle to cycle (eg HU Aqr, Bridge et al 2002 and EP Dra, Bridge et al 2003).

In the case of EP Dra, which has an orbital period of 104.8 min, Bridge et al (2003) attributed the varying eclipse profile to a variation in the amount and location of bright material in the accretion stream. They also found a depression or ‘trough’ like feature starting at $\phi \sim 0.9$ in some cycles. Bridge et al proposed that the accretion material makes a wide accretion curtain which feeds many magnetic field lines before accreting onto the white dwarf. This should result in the X-ray pre-eclipse spectrum being harder than the post-eclipse spectrum.

EP Dra was included in the *XMM-Newton*-MSSL survey of polars (Ramsay & Cropper 2003). The integrated bright phase fluxes in the soft and hard X-ray bands have already been presented by Ramsay & Cropper (2004) who showed that it had a spectrum consistent with the standard accretion model of Lamb & Masters (1979) and King & Lsota (1979). Here we present energy resolved light curves and phase resolved spectroscopy of EP Dra with an emphasis on determining how the absorption varies through the orbital cycle.

2 OBSERVATIONS

EP Dra was observed using *XMM-Newton* (Jansen et al 2001) on 2002 October 18 (*XMM-Newton* orbit 523), approximately two years after the optical observations of Bridge et al (2003). A summary of the observations is given in Table 1. The EPIC-MOS (Turner et al 2001) start time is earlier than that of the EPIC-pn (Strüder et al 2001), and the observation is slightly longer in duration. Observations with the Optical Monitor (Mason et al 2001) were carried out in three filter bands: the V-band, UVW1 (2400–3400 Å) and UVW2 (1800–2400 Å).

Instrument	Mode	Filter	Duration
EPIC MOS 1	Partial window	Thin	18005 s
EPIC MOS 2	Partial window	Thin	18022 s
EPIC PN	Large window	Thin	17670 s
OM	Fast Mode	V	4399 s
OM	Fast Mode	UVW1	4400 s
OM	Fast Mode	UVW2	4399 s
OM	Fast Mode	UVW2	1800 s

Table 1. *XMM-Newton* observation summary for EP Dra from 2002 October 18.

The source counts were extracted from an aperture of 29" for the EPIC-pn and 44" for the EPIC-MOS, centred on the source, and the backgrounds were extracted from annuli around the source aperture of radii 98" for EPIC-pn and 147" for EPIC-MOS (the particle background increased toward the end of the observation). The data were processed using the *XMM-Newton* Science Analysis Software version 5.4. At its brightest point ($\phi \sim 0.78$), the *V*-band magnitude is 16.6. This is comparable with that of $V \sim 17$ of Schwape & Mengel (1997) and the optical observations of Bridge et al (2003) indicating that EP Dra was in a similar, high, accretion state.

3 LIGHT CURVES

The X-ray light curves cover nearly three complete cycles of EP Dra. Figure 1 shows the light curve in the 0.15–10keV energy band for data taken using both the EPIC-pn and combined EPIC-MOS(1+2), together with the OM data. The X-ray data is of a much higher signal to noise and time resolution compared to the *ROSAT* observations of EP Dra presented by Schlegel & Mukai (1995) and Schlegel (1999).

3.1 X-ray

EP Dra shows a distinct bright phase lasting $\Delta\phi \sim 0.6$. This indicates that the observable accretion region is located in the upper hemisphere of the white dwarf, or if located in the lower hemisphere it is spatially extended. The approximate centre of the bright phase is cut by the eclipse of the accretion region and rest of the white dwarf by the secondary star (the count rate at eclipse is consistent with zero): the nature of the eclipse is discussed below.

The phase-folded light curves are split into two energy bands which correspond to the energy ranges 0.15–0.5keV and 2–10keV (Figure 2). The hard X-rays emitted from the accretion region are expected to be optically thin resulting in a light curve which is quasi ‘top-hat’ in form. The fact that the hard X-rays take ~ 0.08 cycles to reach maximum indicate that the accretion region is extended in azimuth on the white dwarf, or has significant vertical height. In soft X-rays there is a steady decrease in flux shortly after reaching maximum flux: by $\phi \sim 0.92$ the flux is consistent with zero. In hard X-rays there is no distinct decrease in flux until $\phi \sim 0.93$ when there is a rapid drop in flux. This is the pre-eclipse dip seen in a number of polars and is attributed to the

accretion stream obscuring our line of sight to the accretion region.

These results are reflected in the softness ratio (Figure 2) which hardens as the bright phase progresses, until at the phase of the main dip there is virtually no observed flux. This is consistent with the proposal of Bridge et al (2003) that there is a wide curtain of material feeding the magnetic field lines in EP Dra.

After the eclipse, where accreting material is not expected to obscure the accretion region to the same extent as the pre-eclipse phase, the energy-resolved light curves are similar to that expected. There are some variations in the softness ratio, but this is probably due to flickering behaviour which is most prominent at softer energies.

3.2 UV and optical

The eclipse phase interval is seen in the UVW1 and UVW2 observations but not in the *V*-band observation. During the eclipse, both UV filters show a count rate consistent with zero during the eclipse. Moreover, the pre-eclipse dip is reflected by a decrease in the UV count rate in both UV filters (Figure 2).

Outside of the eclipse the intensity variation is consistent with the origin being a combination of the heated surface of the white dwarf and the accretion stream. The *V*-band shows a strong rise in brightness at $\phi \sim 0.74$, which is consistent with the rise in X-rays, and is most likely caused by cyclotron emission from the post-shock stream material (Schwape & Mengel 1997). The decrease in brightness post-eclipse is more gradual, starting around $\phi \sim 0.3$ and ending around $\phi \sim 0.34$, again consistent with the end of the bright phase in X-rays.

3.3 The eclipse

The time system for *XMM-Newton* data is Terrestrial Time (TT). We therefore convert the time zero of the ephemeris of Schwape & Mengel (1997) to units of TT. When we fold the barycentrically corrected *XMM-Newton* data on the ephemeris of Schwape & Mengel (1997), we find that the eclipse is offset from $\phi=0.0$, with the eclipse centered at $\phi \sim 0.01$. This is consistent with the optical data of Bridge et al (2003) which also shows an offset. To address this discrepancy, we extracted *ROSAT* HRI data from the public archive and phase each event from EP Dra on the ephemeris of Schwape & Mengel (1997) (after converting the *ROSAT* events times into units of TT). (We did not include the *ROSAT* PSPC data since the source was at a large off-axis angle and was faint). We estimated the mid-point of the eclipse by taking the mean point between the last event seen before eclipse and the first event after eclipse. For the *B* band data of Bridge et al (2003) we estimated the mid-point from the original data rather than their Table 1 which defines the eclipse mid-point as $\phi=0.0$ based on the ephemeris of Schwape & Mengel (1997). We also took the mid-point of eclipse from Remillard et al (1991) and Schwape & Mengel (1997) after converting their times to TT time units and estimated the difference between the observed time of eclipse and the expected time using the ephemeris of Schwape & Mengel (1997). We plot the residuals in Figure 3: this suggests that the period was slightly

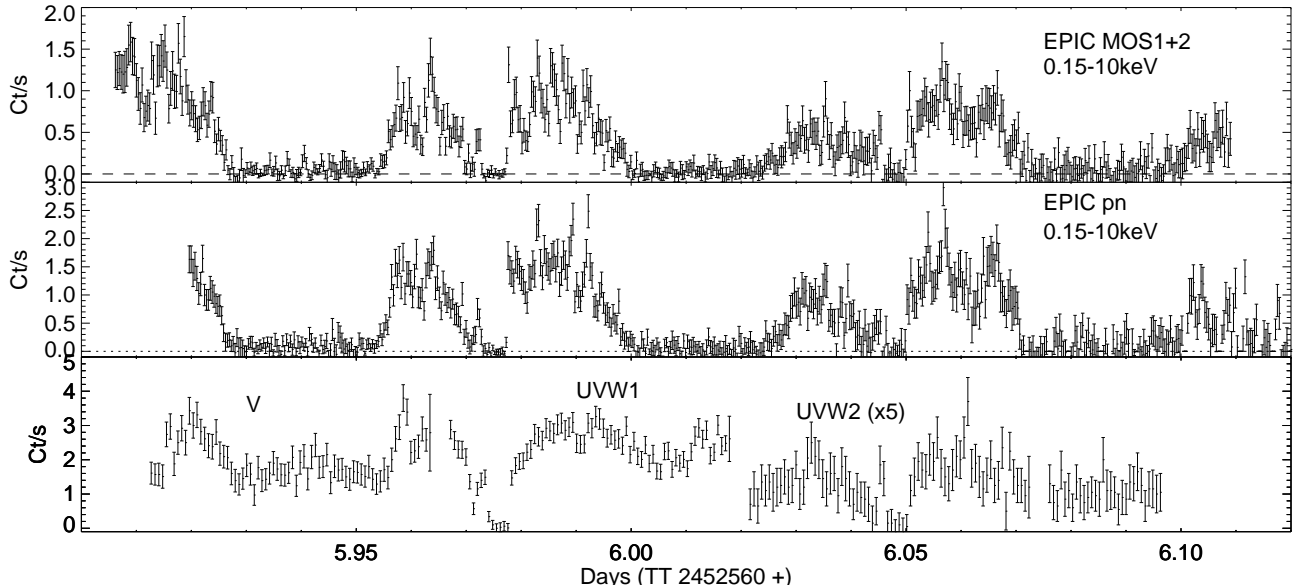


Figure 1. The EPIC-pn, combined EPIC-MOS(1+2) and OM light curves for EP Dra. The X-ray light curves are in 30 s time bins, in the energy range 0.15 – 10 keV. The V -band, UVW1/2 light curves are in 60 s time bins. The X-ray particle background is enhanced in the second half of the observation.

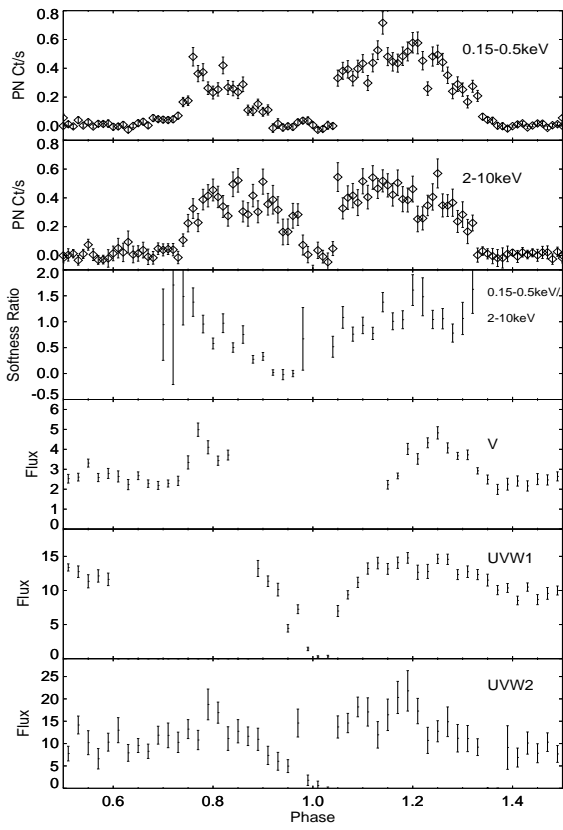


Figure 2. The phase folded and combined EPIC and OM light curves. The EPIC light curves are binned into 100 phase bins; V band 40 sec bins; UVW1 data 30 sec bins; UVW2 60 sec bins and the B band 1 sec bins. The V band and UV fluxes are in units of $\text{erg s}^{-1} \text{cm}^{-2} \text{\AA}^{-1}$.

underestimated by Schwope & Mengel (1997). We find a period of 0.072656272 days (an increase of 0.0011 sec) removes the residuals shown in Figure 3.

We show the *XMM-Newton* and B band data from Bridge et al (2003) corrected so that the eclipse is centered on $\phi=0.00$ in Figure 4. In soft X-rays the phase of eclipse ingress is complicated by the fact that before the eclipse the accretion stream obscures the accretion region. In the B band evidence for the eclipse starts at $\phi=0.961$: this is in contrast to the UV and hard X-rays where the eclipse is not seen for another ~ 50 sec. In the UV the eclipse ingress takes less than 5 sec, while in hard X-rays it is more difficult to determine because of the lower count rate, but is less than 20 sec. At eclipse egress, the B band flux starts to increase before the UV or X-ray emission. However, the B band egress finishes at the same phase at which the UV and X-ray emission appears. In the UV and soft X-ray band the egress is very sharp, taking ~ 5 sec. In hard X-rays the rise time is more uncertain, but similar. This demonstrates the difficulty of determining the eclipse centers in different energy bands. In the optical the ingress and egress marks the eclipse of the white dwarf, while in the X-ray band it marks the eclipse of the accretion region which can be anywhere on the surface of the white dwarf.

Using the standard Roche lobe geometry we can estimate the mass of the white dwarf assuming a mass ratio, $q = M_2/M_1$. Using the standard period-secondary-mass relationship for main sequence stars (cf Warner 1995) we estimate $M_2 \sim 0.19M_{\odot}$ for EP Dra. For inclinations of 78° , 80° and 82° we find $M_1=0.50$, 0.68 and $0.95M_{\odot}$ respectively. Schwope & Mengel (1997) determine $M_1=0.43M_{\odot}$ from optical spectroscopy measurements.

4 SPECTRA

It is clear from Figure 2 that the pre-eclipse bright phase is more absorbed than the post-eclipse bright phase. To place this on a more quantitative level, we combined single and double events and extracted spectra from the pre-eclipse ($\phi=0.75$ –0.95) and post-eclipse ($\phi=0.05$ –0.25) bright

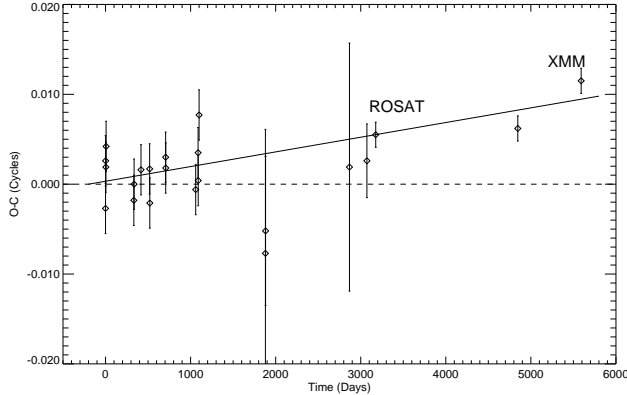


Figure 3. The O-C diagram for the eclipse center based on data presented in Remillard et al (1991), Schwone & Mengel (1997), Bridge et al (2003), the XMM-Newton data here and *ROSAT* HRI data extracted from the archive. We used the ephemeris of Schwone & Mengel (1997) to calculate the expected time of eclipse center. The fit to these times is shown by a straight line. This suggests the period is slightly greater than that estimated by Schwone & Mengel.

	Pre-eclipse	Post-eclipse
$N_{H,1}$ (10^{20} cm $^{-2}$)	$1.1^{+0.5}_{-0.4}$	$0.0^{+0.2}_{-0.1}$
$N_{H,2}$ (10^{22} cm $^{-2}$)	$3.0^{+0.6}_{-0.5}$	$2.8^{+0.6}_{-0.5}$
cvf, ₂	$0.87^{+0.01}_{-0.02}$	$0.79^{+0.01}_{-0.02}$

Table 2. The absorption parameters for X-ray spectra taken pre and post eclipse. The first component is a neutral absorption component while the second component is a neutral absorption component with a partial covering fraction (cvf).

phases. Only the first two cycles were used as the particle background was much greater in the third. The spectrum was fitted using the XSPEC (Arnaud 1996) spectral analysis package and the epn_ff20_sdY9_thin.rsp response matrix. For details of the X-ray spectra of polars observed in a high accretion state in general and the energy balance of EP Dra in particular see Ramsay & Cropper (2004). Here we investigate the specific question as to whether the absorption is greater before eclipse compared to after it.

We fitted the spectra using the stratified accretion emission model of Cropper et al (1999) plus a blackbody component and a Gaussian at 6.4keV. We also added a neutral absorption component and a neutral absorption component with partial covering. These parameters were allowed to vary between the pre and post eclipse spectra, while the emission parameters were tied. We fitted both spectra simultaneously. A reasonably good fit was obtained ($\chi^2_{\nu}=1.48$, 144dof). The residuals are likely to be due to the fact that the spectrum is intrinsically varying over the phases over which the spectra were accumulated (cf the softness ratio, Figure 2). We show the spectra in Figure 5 and the absorption parameters in Table 2. This shows that the pre-eclipse spectrum is more absorbed than the post-eclipse spectrum.

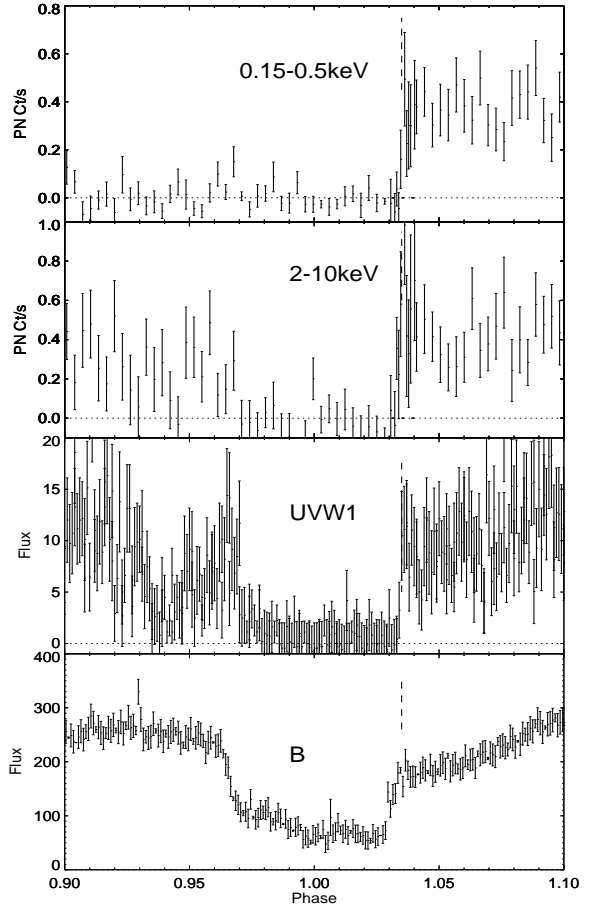


Figure 4. The eclipse phase interval. From the top: the soft and hard X-ray data from XMM-Newton; the UVW1 data from XMM-Newton and *B* band data taken from Bridge et al (2003). The top two panels have bins sizes of 20 sec, apart from the phase interval $\phi=0.04-0.05$ which is binned into 5 sec bins. The UVW1 and *B* band data 5 sec. The phase of egress in the X-ray and UV bands ($\phi=0.034$) is shown as a dashed vertical line.

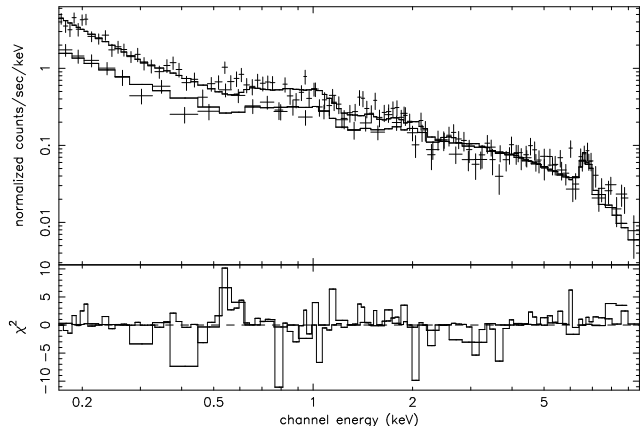


Figure 5. The post-eclipse bright phase spectrum (upper set of crosses) with best-fit model (upper solid line) and residuals; The pre-eclipse bright phase spectrum (lower set of crosses) with best-fit model (lower solid line) and residuals.

5 ABSORPTION IN THE ACCRETION STREAM

The soft X-ray light curve (Figure 2) shows a general and gradual decrease in flux from the start of the bright phase, leading up to a prominent dip when the flux is consistent with zero. In hard X-rays there is a sudden drop in flux to the pre-eclipse dip. This implies that while the accretion flow becomes attached over a wide range of magnetic field lines (Bridge et al 2003), there is a dense, well defined, ‘core’ of absorption. What makes EP Dra unusual is the depth of the dip in the hard band, implying that the dense core has an unusually high column depth.

Ramsay et al (2004) estimated the depth of the absorption column in GG Leo and found that it was different depending on whether it was determined using soft X-rays or in the UV. To estimate the absorption column that would be needed to produce the observed drop in count rate (the mean count rate in each band between $\phi=0.93-0.97$), we took the pre-eclipse spectrum (§4) and increased the absorption column to obtain the observed decrease in count rate for soft X-rays, hard X-rays and the UV bands. For the X-ray data we increased the neutral absorption model component, while for the UV data we used the UVRED model within XSPEC (this is necessary as the neutral absorber model component does not extend to UV energies). We use the relationship between optical extinction and total absorption column of Bohlin, Savage & Drake (1978). We note that this is likely to be a lower limit since the UVRED model assumes a large fraction of the UV absorption is caused by dust, which is unlikely to be present in the accretion stream. We find we need a column depth of $1-2 \times 10^{21} \text{ cm}^{-2}$ in the UV bands, $8 \times 10^{20} \text{ cm}^{-2}$ for 0.15–0.5keV and $1 \times 10^{23} \text{ cm}^{-2}$ for 2–10keV bands: they are clearly inconsistent.

A solution may be that different absorption components should be applied to the various emission components. This is not surprising since the line of sight to the reprocessed emission site (which produces a significant fraction of the soft X-ray flux, Ramsay & Cropper 2004) will be different to the line of sight to the post-shock accretion region (which produces all of the harder X-rays). The UV emission, will again have a different line of sight. However, almost all investigators when fitting X-ray spectra of polars have modelled their spectra assuming that the same absorption component can be used to model the absorption of each of the emission components.

To investigate this further, we fitted the post-eclipse spectrum with a model which applied separate absorption components to the blackbody and the stratified emission region and also a model which applied the same absorption model to both emission components (as in §4). We applied one neutral absorption component to both to account for interstellar absorption. We find that the former (physically more realistic) model gives a better fit ($\chi^2_\nu=1.33$, 92dof) compared to the latter model ($\chi^2_\nu=1.53$, 94dof) at a significance level of greater than 99.9 percent. Further, we find that the blackbody emission component requires one absorption component, while the stratified emission region component requires two absorption components (with different column densities and covering fractions).

Ramsay et al (2004) determined the mass of the white dwarf in 3 polars using XMM-Newton data the same strat-

ified emission model as used here. They found that if they restricted the energy range to 3–10keV rather than the full 0.2–10keV range they determined less massive white dwarfs. This was due to the fact that absorption plays an important role at lower energies and therefore there may be some degeneracy between the level of absorption and the slope of the stratified emission model. However, Ramsay et al (2004) also noted that the fits to the 3–10keV spectra were poorer compared to the fits made using the full energy range and suggested that this may be due to the absorption being more complex than applying the same absorption model to both the blackbody and stratified emission models. Here we find that separate absorption models should be applied to each emission component. This would have implications for the resulting mass of the white dwarf.

6 LOCATION OF ACCRETION STREAM MATERIAL

As the accretion flow leaves the secondary star it falls under gravity towards the white dwarf until the magnetic pressure of the white dwarf balances the ballistic pressure of the in-falling material. In reality a treatment of the transition between the ballistic and the magnetic dominated region is not simple. Different parts of the accretion stream material will therefore satisfy this condition at different points along the ballistic trajectory. The actual location of threading for a particular part of the accretion stream will depend upon the density of the material, and the orientation of the magnetic field lines relative to the in-falling material. This means that the material will not all be threaded by the magnetic field at the same point (see, for example, Liebert & Stockman 1985, Mukai 1988, Heerlein, Horne & Schworer 1999).

Evidence for material being coupled on to field lines covering a range in magnetic azimuth has long been available (eg Ferrario, Tuohy & Wickramasinghe 1989). These XMM-Newton observations show that in EP Dra, the extent in phase of the soft X-ray absorption seen prior to the eclipse centre indicates that the accretion stream attaches onto a wide range of magnetic field lines of the white dwarf and is able to obscure the X-ray emission site for a significant fraction of the orbit. The stream does, however, have a dense and well defined core. In contrast, in HU Aqr, Schworer et al (2001) show that material is accreted over a narrower range of azimuth.

The fact that the main stream dip is located very shortly before the eclipse, $\phi \sim 0.944$ or an azimuth of $\sim 20^\circ$, implies that the most dense part of the stream becomes attached to the magnetic field lines at a point relatively distant from the white dwarf. We can compare this to the phase of the prominent dip seen in HU Aqr. This has been extensively observed using X-ray instruments and the azimuth of the main dip has been seen to vary from $34-50^\circ$. This implies that the main accretion stream in EP Dra is coupled by the magnetic field further from the white dwarf compared to HU Aqr. In the standard accretion flow model the point at which the stream gets attached by the magnetic field is the point at which the magnetic pressure equals the ram pressure of the stream (cf Mukai 1988). The location of this point is thought to be relatively weakly dependent on the mass transfer rate

and the mass of the white dwarf. It is more likely to be dependent on the magnetic moment ($\mu = BR_{wd}^3$) of the white dwarf and the angle that the magnetic axis makes with the spin axis of the white dwarf, β .

The magnetic field strength of the white dwarf in HU Aqr is 36MG (Glenn et al 1994) while in EP Dra it is 16 MG (Schwope & Mengel 1997). For the coupling point to be further from the white dwarf in EP Dra compared to HU Aqr this would imply that the white dwarf in EP Dra is significantly less massive (larger radii and hence greater μ) compared to HU Aqr. In §3.3 we estimate $M_1=0.50M_\odot$ for an inclination of 78° – this compares with $M_1=1M_\odot$ for HU Aqr (Schwope et al 2001).

For high angles of β , the stream travels further before it feels the effect of the magnetic field. Support for a high β angle in EP Dra may be found in the peak of the X-ray bright phase: with the eclipse center fixed on $\phi=0$, the center of the hard X-ray bright phase (defined as the mid point between the rise and end of the bright phase) is $\phi=0.02$. This implies the accretion region is behind the line of centers joining the two stars. This is unusual since Cropper (1988) found that in most systems the bright phase leads the secondary and has a mean azimuth of $\sim 20^\circ$. High signal to noise polarimetric data should be able to determine the co-latitude of the accretion region.

7 CONCLUSIONS

We have presented X-ray energy resolved and optical/UV light curves of the eclipsing polar EP Dra. They show a prominent dip in X-rays and in the UV which is due to the accretion stream obscuring the accretion region on the white dwarf. Our modelling of the X-ray spectra taken before and after the eclipse of the secondary provides evidence that accretion material attaches on to the magnetic field lines along a wide arc along the ballistic trajectory supporting the suggestion of Bridge et al (2003).

We find that the level of absorption needed to account for the pre-eclipse absorption dip is much greater in hard X-rays compared to softer X-rays. We suggest that one factor which may cause this effect is that the line of sight to the emission sites producing soft X-rays, hard X-rays and UV is different. We test this by fitting such a model to the X-ray data and find that a better fit is achieved compared to using an absorption model which is applied to both emission components. This has implications for fits to the continuum spectra of polars.

8 ACKNOWLEDGMENTS

This is work based on observations obtained with *XMM-Newton*, an ESA science mission with instruments and contributions directly funded by ESA Member States and the USA (NASA). We thank the referee for helpful comments.

REFERENCES

Arnaud K. A., 1996, Astronomical Data Analysis Software and Systems V, eds. Jacoby G. and Barnes J., p17, ASP Conf. Series volume 101.

Bohlin, R. C., Savage, B. D., Drake, J. F., 1978, ApJ, 224, 132

Bridge, C., Cropper, M., Ramsay, G., Perryman, M. A. C., de Bruijne, J. H. J., Favata, F., Peacock, A., Rando, N., Reynolds, A. P., 2002, MNRAS, 336, 1229

Bridge, C. M., Cropper, M., Ramsay, G., de Bruijne, J. H. J., Reynolds, A. P., Perryman, M. A. C., 2003, MNRAS, 341, 863

Cropper, M., 1988, MNRAS, 231, 597

Cropper, M., Wu, K., Ramsay, G., Kocabiyik, A., 1999, MNRAS, 306, 684

Ferrario, L., Tuohy, I. R., Wickramasinghe, D. T., 1989, 341, 327

Glenn, J., Howell, S. B., Schmidt, G. D., Liebert, J., Grauer, A. D., Wagner, R. M., 1994, ApJ, 424, 967

Heerlein, C., Horne, K., Schwope, A. D., 1999, MNRAS, 304, 145

Jansen F., et al, 2001, A&A, 365, L1

King, A. R., Lasota, J. P., 1979, MNRAS, 188, 653

Lamb, D. Q., Masters, A. R., 1979, ApJ, 234, 117

Liebert, J., Stockman, H. S., 1985, In *Cataclysmic Variables and Low Mass X-ray binaries*, ed. Lamb, D. Q., Patterson, J., Reidel, p.151

Mason, K. O., et al 2001, A&A, 365, L36

Mukai, K., 1988, MNRAS, 232, 175

Ramsay, G., Cropper, M., 2003, In Proc Cape Town Workshop on mCVs, astro-ph/0301609

Ramsay, G., Cropper, M., 2004, MNRAS, 347, 497

Ramsay, G., Cropper, M., Mason, K. O., Cordova, F. A., Priedhorsky, W., 2004, MNRAS, 347, 95

Remillard, R. A., Stroozas, B. A., Tapia, S., Silber, A., 1991, ApJ, 379, 715

Schlegel, E. M., Mukai, K., 1995, MNRAS, 274, 555

Schlegel, E. M., 1999, ApJ, 117, 2494

Schwope, A. D., Mengel, S., 1997, Astron Nachr, 318, 25

Schwope, A. D., Schwarz, R., Sirk, M., Howell, S. B., 2001, A&A, 375, 419

Strüder, L., et al, 2001, 365, L18

Turner, M., et al 2001, A&A, 365, L27

Warner B., 1995, *Cataclysmic variable stars*, Cambridge Univ. Press, Cambridge